Toward Green Ferroalloys: Replacement of Fossil Reductants in the Pre-reduction Process of Chromite by Bio-Based Alternatives

M. Sommerfeld and B. Friedrich

Abstract The production of ferrochrome via carbothermic reduction in submerged arc furnaces is an energy-intensive process relying on the usage of coal and coke as reducing agents. The pre-reduction of chromite in a rotary kiln is currently carried out to decrease the specific electric energy consumption in the smelting furnace. However, as fossil reductants are still needed for reduction, CO_2 is emitted. The usage of bio-based carbon with a faster carbon cycle compared to fossil reductants could be an option to decrease the specific CO_2 footprint of Ferrochrome production. In this paper, the pre-reduction of chromite was investigated using various bio-based reducing agents and lignite coke as a fossil reference. Isothermal reduction trials were conducted at 1000, 1150, and 1300 °C and different holding times. While at lower temperatures the pre-reduction was insufficient, the bio-based reducing agents yield a degree of reaction between 61.0% and 65.4% at 1300 °C reaction times of 360 min. The highest degree of reaction is reached using coconut charcoal, followed by corn, olive, and bamboo charcoal. Coke results in the lowest degree of reaction with 51.9%. While the bio-based reducing agents performed similar after long reaction times, significant deviations were observed for shorter reaction times. X-ray diffraction was carried out to investigate the obtained product, which showed that the pre-reduction was mostly due to the formation of carbides, while the intensity of metals in the sample was rather low.

Keywords Pyrometallurgy · Sustainability · Ferroalloys · Ferrochrome · Pre-reduction

M. Sommerfeld (✉) · B. Friedrich
IME Process Metallurgy and Metal Recycling, Institute of RWTH Aachen University, Intzestraße 3, 52056 Aachen, Germany
e-mail: msommerfeld@ime-aachen.de

A. Lazou et al. (eds.), *REWAS 2022: Developing Tomorrow's Technical Cycles (Volume I)*, The Minerals, Metals & Materials Series,
https://doi.org/10.1007/978-3-030-92563-5_65

Introduction

The usage of fossil-reducing agents for the production of ferroalloys leads to the direct emission of CO_2. The production of ferrochromium solely was responsible for the emission of at least 15.5 million tons of CO_2 in 2016 due to the usage of reducing agents [1]. One option to reduce the emission of CO_2 could be the usage of bio-based carbon, which can be considered CO_2-neutral, if the same amount of biomass is recultivated, that is consumed [2]. Especially the iron and steel industry carried out a considerable amount of research regarding the usage of bio-based carbon [3–11], while less research was carried out considering the substitution of fossil carbon by bio-based carbon in the ferroalloy industry [1]. For the production of high carbon ferrochrome, several processes are currently industrially carried out: the smelting of chromite in open, semiclosed, or closed alternating current (AC) submerged arc furnaces (SAF), the smelting in open arc direct current (DC) furnaces and the pre-reduction of chromite in a rotary kiln followed by smelting in closed AC SAFs. The pre-reduction AC SAF process has two advantages: together with the DC furnace it has the highest chromium recovery, and has the lowest specific electric energy consumption (SEC) per ton of FeCr [12]. Therefore, the pre-reduction process is considered a viable option especially for countries with unsteady electricity supply or high prices for electric energy. Especially in recent years, a significant amount of research was carried out investigating the pre-reduction process of chromite [13–21]. Kleynhans et al. [14] determined, that the SEC decreases depending on the pre-reduction as shown in Eq. 1 [14].

$$\mathrm{SEC/(kWh/t)} = 3403.7\ \mathrm{kWh/t} - 21.5\ \mathrm{kWh/t} \cdot \mathrm{pre{-}reduction/\%} \quad (1)$$

Experimental

In this section, the used raw materials and methods are described.

Materials

In this study, a Turkish metallurgical-grade chromite concentrate (following named chromite) is used as a raw material. The chemical composition of the chromite ore determined by x-ray fluorescence spectroscopy (XRF) is shown in Fig. 1. A detailed characterization of the ore is presented elsewhere [22].

In addition, it was determined by Mössbauer spectroscopy, that 74% of iron is ferrous iron and 26% is ferric iron. These findings allowed the calculation of the amount of oxygen bound to iron and chromium, which must be removed in the

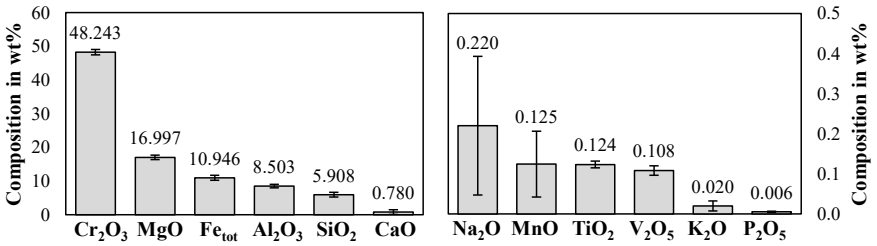

Fig. 1 Bulk chemical analysis of the used chromite sample

pre-reduction of chromite. The oxygen content that has to be removed is therefore 18.779 wt% in the chromite. Assuming that carbon will react completely with chromium- and iron oxide to carbon monoxide, 14.805 g of carbon per 100 g chromite are the stoichiometric carbon addition to remove oxygen bound to chromium and iron completely.

As reducing agents, charcoal made from coconut shells (following named coconut), corn cobs (following named corn), olive pomace (following named olive), bamboo (following named bamboo), and lignite coke made from Rhenish lignite (following named coke) are used. To calculate the required addition of reducing agents, it is necessary to determine the carbon content in each reducing agent. Table 1 shows the proximate-, ultimate-, P- and Cl-analysis of the reducing agents investigated in this study. For the calculation of the necessary addition of carbon, the carbon content as determined by the ultimate analysis is used.

According to the analysis shown in Table 1, the bio-based reducing agents have a significantly lower sulfur content compared to fossil coke, which is beneficial, since sulfur is an impurity in ferroalloys. However, the chlorine content of the bio-based reducing agents is higher compared to the chlorine content in coke, especially corn charcoal and olive charcoal have a high chlorine content. In an industrial operation,

Table 1 Proximate-, ultimate- and Cl-analysis of bio-based charcoal and coke used

All in wt%	Proximate analysis				Ultimate analysis					
Reducing agent	Fixed carbon	Total moisture	Ash	Volatile matter	C	H	N	S	O	Cl
Coconut charcoal	72.1	8.7	7.2	12.1	73.84	1.24	0.39	0.06	8.60	0.07
Corn charcoal	81.3	4.6	4.8	9.3	81.62	2.30	0.63	0.04	5.99	0.51
Olive charcoal	63.7	7.2	12.6	16.4	67.54	1.60	1.16	0.05	9.79	0.43
Bamboo charcoal	80.4	11.6	3.9	4.1	79.73	1.21	0.40	0.08	3.12	0.12
Lignite coke	87.5	0.5	9.0	3.0	89.0	0.4	0.4	0.5	0.7	0.03

Table 2 Ash analysis and basicity of bio-based charcoal and coke used

Reducing agent	Ash composition in wt%								Basicity
	Al_2O_3	CaO	Fe_2O_3	K_2O	MgO	Na_2O	P_2O_5	SiO_2	
Coconut charcoal	4.1	23.0	4.1	7.7	3.6	2.9	1.6	46.8	0.8
Corn charcoal	0.6	1.8	1.5	46.1	3.4	< 0.01	6.4	15.8	3.2
Olive charcoal	2.2	16.8	2.0	34.2	3.4	1.6	7.1	8.0	5.7
Bamboo charcoal	2.8	2.8	3.1	35.6	3.9	< 0.01	6.3	30.6	1.4
Lignite coke	3.1	35.4	10.9	0.8	15.8	6.7	0.2	2.2	13.1

this could lead to severe corrosion of equipment in contact with off-gas. Besides sulfur, further impurities could be introduced in the process from the ash. Therefore, the ash was further analyzed. Samples of the reducing agents weighing 100 g are burned in an oxidizing atmosphere at 815 °C until a constant mass is reached. Afterward, the ash is analyzed by XRF. Table 2 shows the determined chemical composition of the ash reported as oxides and the basicity of the ash samples as calculated by Eq. 2.

$$\mathrm{B} = \frac{wt\%_{\mathrm{cao}} \cdot wt\%_{\mathrm{Fe_2O_3}} \cdot wt\%_{\mathrm{MgO}} \cdot wt\%_{\mathrm{Na_2O}} \cdot wt\%_{\mathrm{K_2O}}}{wt\%_{\mathrm{SiO_2}} \cdot wt\%_{\mathrm{Al_2O_3}}} \tag{2}$$

Noticeable is the high CaO and MgO content in lignite coke, which results in the highest basicity of the lignite coke ash. In corn, olive, and bamboo ash, the prevalent compound is K_2O. Even though the analysis is reported as oxides, based on the high chlorine content in the samples shown in Table 1, potassium might be present at least partially as potassium chloride, which was also indicated by x-ray diffraction of the ash not presented in this article. The dominant component in coconut charcoal is SiO_2, yielding ash with the lowest basicity. During the smelting process after pre-reduction, the major oxides Al_2O_3, CaO, MgO, and SiO_2 from the ash will accumulate in the slag phase, while potassium and sodium will partially be volatilized during smelting as well. Especially since the potassium content in the biomass is quite high, this could lead to disadvantages during processing, like increased refractory corrosion. Iron oxide will be reduced either during pre-reduction or smelting as well as phosphorous, which is mostly transferred into the metal and partially into the slag. As phosphorous is an impurity in ferroalloys, this is another challenge to overcome, since all investigated ash samples contained more phosphorous than lignite coke.

Chromite was used in the trials as received and not pre-treated, while the reducing agents were ground in a vibratory disk mill for 20 s each. Table 3 shows the particle size of the raw materials as determined by dynamic imaging analysis.

While coconut, olive, and bamboo have a similar particle size, the same grinding time yielded finer corn charcoal and a coarser coke.

Table 3 Percentile particle sizes of raw materials used in this study

Raw material	Chromite	Corn charcoal	Coconut charcoal	Olive charcoal	Bamboo charcoal	Lignite coke
$x_{10,3}$ in µm	86.9	4.6	5.0	4.9	5.1	8.7
$x_{50,3}$ in µm	192.2	16.7	21.7	23.3	25.9	42.8
$x_{90,3}$ in µm	371.8	69.6	78.8	78.8	82.0	87.6

Methods

Mass loss trials were carried out using a Nabertherm HT 16/18 high-temperature furnace equipped with molybdenum disilicide heating elements. The initial sample mass per trial was 35.00 g, mixtures of ore with stoichiometric, sub-stoichiometric, and over-stoichiometric additions of reductants were investigated. The mass loss after every trial was measured, to determine the degree of reaction. Ore and reductants were also heated separately, to determine the individual mass loss without reduction reactions. The samples were placed in alumina crucibles (Ø = 50mm, h = 75mm) with a purity of 99.7%. To prevent oxidation of the samples, the furnace chamber was continuously flushed with 5 Nl/min argon in every part of the trial. The volume of the furnace chamber was 16 l. A maximum of six crucibles were placed inside the furnace per trial, to ensure that the temperature of the samples was uniform. Variable heating parameters in this investigation were the maximum temperature of each trial and the holding time at the maximum temperature. The heating time from room temperature to the maximum temperature was 3.5 h and the cooling time was not controlled. However, in the first hour after the trial, the furnace chamber cooled down by roughly 400 °C and in the subsequent hour by 200 °C.

To evaluate the degree of reaction, the mass loss based on the reduction was calculated using Eq. 3 subtracting the weight loss of the ore sample and reductant individually from the mass loss of the ore-reductant mixture. To consider the varying amount of ore and reductants in the mixtures, the mass loss of the pure compounds was calculated using Eq. 4. Finally, the degree of reaction was calculated per 100 g of chromite using Eq. 5. The maximum mass loss Δm_{Max} assumes, that oxygen bound to chromium and iron is completely removed as carbon monoxide. Based on the composition presented in Fig. 1, the maximum mass loss Δm_{max} per 100 g ore would be 32.863 g including oxygen removed from the ore and the removal of added carbon as carbon monoxide.

$$\Delta m_{\text{Reduction}} = \Delta m_{\text{Mixture}} - \Delta m_{\text{Pure Compounds}} \tag{3}$$

$$\Delta m_{\text{Pure Compounds}} = \frac{\Delta m_{\text{Chromite}}}{m_{\text{Mixture}} / m_{\text{Chromite}}} + \frac{\Delta m_{\text{Reductant}}}{m_{\text{Mixture}} / m_{\text{Reductant}}} \tag{4}$$

$$\text{Degree of Reaction} = 100\% \cdot \frac{\Delta m_{\text{Reduction}} \cdot 100\,\text{g} \,/\, m_{\text{Chromite}}}{\Delta m_{\text{Max}}} \tag{5}$$

Before the experimental work a thermochemical simulation of the pre-reduction process was carried out using the commercial modeling software FactSage™ 8.0 [23]. For the simulation the chromite composition presented in Fig. 1 including the ferric and ferrous ratio determined by Mössbauer spectroscopy was used, while carbon was used as the reducing agent. The databases FToxid, FactPS, and SGTE were used for the simulation. In contrast to Eq. 5, the removed oxygen per 100 g chromite was calculated by Eq. 6. The total mass of oxygen according to the simulation was used. The maximum amount of oxygen is based on the amount of oxygen bound to chromium and iron and is 18.779 g.

$$\text{Removed Oxygen} = 100\% \frac{\text{Mass of Oxygen in Atmosphere}}{m_{\text{Maximum Oxygen Removed}}} \tag{6}$$

Samples after the direct reduction of chromite and the initial ore were analyzed by x-ray diffraction with a "STADI MP" powder diffractometer made by "STOE&Cie GmbH" using the Kα1-radiation of molybdenum (wavelength = 0.70930Å). For the evaluation, HighScore Plus 4.9.0.27512 and the PDF-4 Axiom 2021 database were used.

Results and Discussion

In this chapter, the results of the thermochemical simulation, the experimental trials, the phase analysis of the reduced samples and the potential specific electrical energy saving are presented.

Thermochemical Simulation

Figure 2 shows the removed oxygen as calculated by Eq. 6 based on the thermochemical simulation in dependence of the temperature and the carbon addition.

According to Fig. 2, at temperatures below 1100 °C, a plateau is reached after the removal of 15–20% oxygen, which is mostly due to the reduction of iron oxides. At 1150 °C and 1200 °C, more oxygen is removed as chromium oxides start to react and a $(Cr, Fe)_7C_3$ phase is formed. However, a significant amount of chromium is still bound in a spinel phase. Above 1250 °C, the amount of the spinel phase and the chromium concentration is significantly reduced, in addition to the $(Cr, Fe)_7C_3$ phase, a $(Cr, Fe)_3C_2$ phase is formed in equilibrium with graphite. To examine the behavior of iron and chromium and iron more closely, Fig. 3 shows how iron and chromium are bonded at 1300 °C depending on the amount of carbon added.

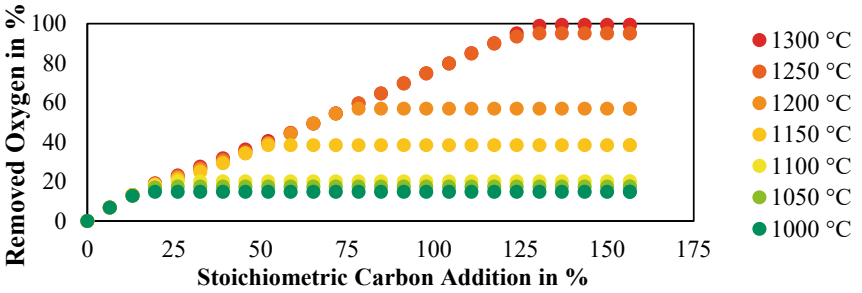

Fig. 2 Removed oxygen, dependent on the temperature and carbon addition

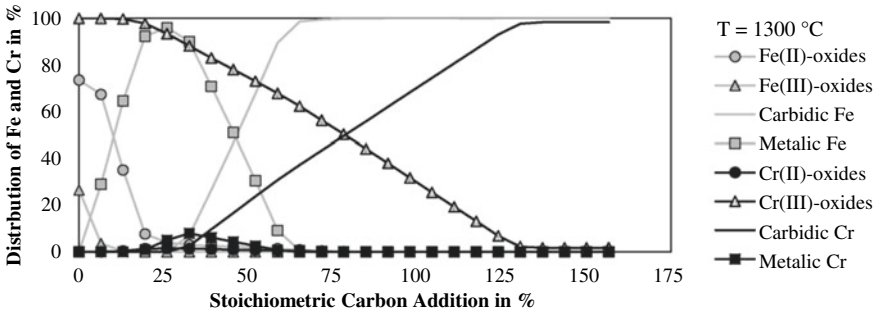

Fig. 3 Bonding of iron and chromium dependent on the carbon addition at 1300 °C

According to Fig. 3, adding 6.5% of the stoichiometric carbon requirement already leads to the formation of 29% iron in a metallic state, while trivalent iron oxides are reduced nearly completely. Adding 26% of carbon nearly reduces divalent iron completely and 5% of chromium is reduced into a metallic solution phase as well. Adding more carbon results in the reduction of chromium and $(Cr, Fe)_7C_3$ starts to form. In addition, metallic iron reacts to carbides as well. When the carbon addition exceeds 78.3%, no metallic phases are present anymore and iron and chromium are either bound as $(Cr, Fe)_7C_3$ or oxides. Above carbon additions of 130.5%, in addition to the $(Cr, Fe)_7C_3$ phase, a $(Cr, Fe)_3C_2$ phase starts to form and chromium and iron are not reduced anymore. The amount of iron not reduced in equilibrium with graphite is 0.02% and 1.71% of chromium is not reduced.

Degree of Reaction

The degree of reaction based on Eq. 5 was determined for various reducing agents, reaction temperatures and holding times for the solid-state reduction of chromite.

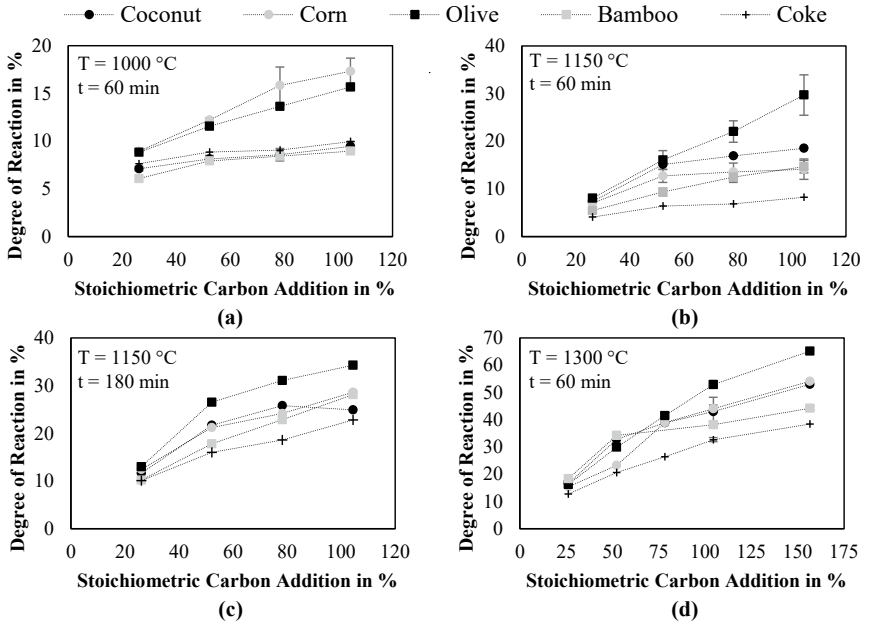

Fig. 4 Degree of reaction dependent on the carbon addition for various reducing agents and temperatures. **a** T = 1000 °C, t = 60 min, **b** T = 1150 °C, t = 60 min, **c** T = 1150 °C, t = 180 min, **d** T = 1300 °C, t = 60 min

Figure 4 shows the degree of reaction for various parameter combinations of preliminary trials.

In most cases, an increasing stoichiometric carbon addition also results in an increased degree of reaction. At 1000 °C using 104.43% carbon in the form of corn charcoal results in a degree of reaction of 17.4%, which is the highest degree of reaction and slightly higher than the theoretical removal of oxygen shown in Fig. 2. Olive charcoal results in a slightly lower degree of reaction, while the other three reducing agents yield a degree of reaction below 10%. Increasing the temperature to 1150 °C using the same holding time of 60 min results in a significant increase in the degree of reaction. At those parameters, olive charcoal yielded the highest degree of reaction. While the other bio-based reducing agents yielded a relatively similar degree of reaction, coke yielded a significantly lower degree of reaction. In Fig. 4c, the holding time is tripled compared to Fig. 4b, which yields a significantly increased degree of reaction for all reducing agents, except olive charcoal, where the degree of reaction increased only slightly. Coke still has the lowest degree of reaction, but is now closer to bamboo charcoal, coconut charcoal, and corn charcoal. In Fig. 4d, the holding time is 60 min again and the temperature is increased to 1300 °C, which increases the degree of reaction using olive charcoal in the best case to 65%, however, a stoichiometric carbon addition of 156.64% was used in this

case. Using only 104.43% carbon yields a degree of reaction of 52.9% using olive charcoal, while the lowest degree of reaction was observed using coke with 32.6%.

As the degree of reaction at low temperatures was insufficient, more trials were carried out at 1300 °C with a constant carbon addition of 104.43% for different holding times. Higher temperatures were not investigated, to avoid partial melting of the mixtures, which could lead to damring formation in the pre-reduction process in rotary kilns [16].

During the first 90 min, olive charcoal yields the highest degree of reaction and coke the lowest. Corn and coconut charcoal behave similarly and slightly better than bamboo charcoal. A further increase in the reaction time especially yields an enhanced reaction for bamboo and coke, whereas the reaction of the other reducing agents increases less strongly. After 360 min, the bio-based reducing agents yield a degree of reaction between 61.0% and 65.4%. The highest degree of reaction is reached using coconut charcoal, followed by corn, olive, and bamboo charcoal. Coke results in the lowest degree of reaction with 51.9%. The lower degree of reaction of coke is in line with comparisons carried out by Kleynhans et al. [15], who investigated several fossil-reducing agents and determined, that the pre-reduction using coke was between 33 and 44%, while anthracite yielded a higher pre-reduction between 56 and 66% [15]. This was explained by the higher volatile content and therefore higher hydrogen content compared to the thermally treated coke [15]. The hydrogen content of the bio-based reducing agents varies between 1.21% and 2.30% and is 0.4% in the fossil coke, based on Table 1. The hydrogen-, and volatile content could be an explanation, why the bio-based reducing agents performed better compared to coke, but those properties cannot be used to explain the reducing ability of the bio-based reducing agents compared to each other. For example, coconut and bamboo have a similar hydrogen content, but they significantly differ in their degree of reaction.

Phase Analysis

To evaluate the solid phases generated in the trials, samples treated for 60 min with a stoichiometric carbon addition of 104.43% at different temperatures were analyzed by X-ray diffraction. In addition, the ore as received was analyzed by X-ray diffraction as well. Figure 6 shows the diffraction patterns of samples reduced with coconut charcoal and coke. Those reducing agents were chosen, as they yielded the highest and lowest degree of reaction as shown in Fig. 5.

Phases selected for the phase analysis were chromium carbide with the chemical formula Cr_7C_3 and the PDF-number 04-007-1045, an α-iron phase containing chromium with the chemical formula $Cr_{0.03}Fe_{0.97}$ and the PDF-number 04-004-2488, forsterite with the chemical formula Mg_2SiO_4 and the PDF-number 00-004-0768 and a magnesiochromite spinel with the chemical formula $Mg_{0.56}Ti_{0.01}Cr_{1.33}Fe_{0.51}Al_{0.59}O_4$ and the PDF-number 04-024-3779. In all reduced samples and in the raw ore, chromite and forsterite were identified. The intensity of chromite was the highest in all samples, however, spinels without chromite have peaks

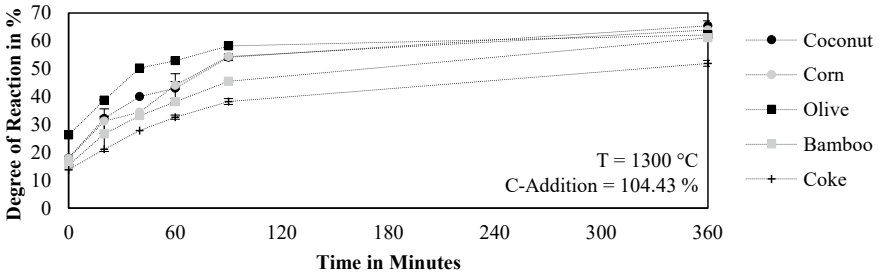

Fig. 5 Degree of reaction dependent on the holding time at 1300 °C for various reducing agents

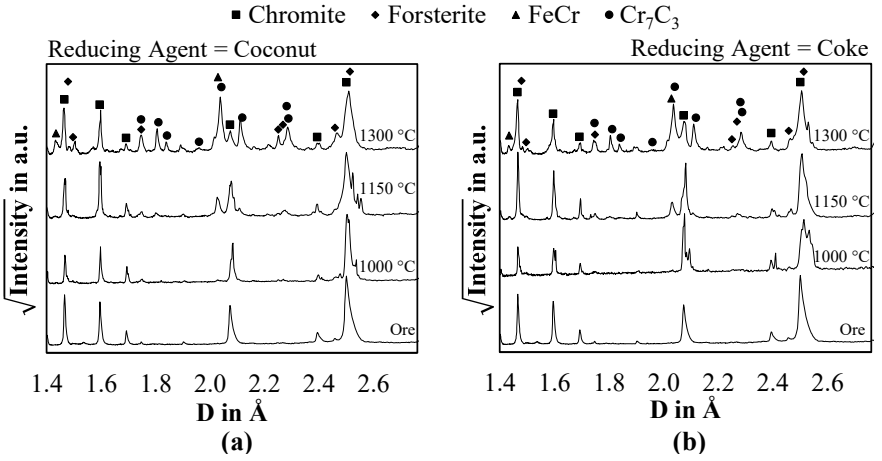

Fig. 6 X-ray diffraction pattern of raw ore and ore reduced at various temperatures with **a** coconut charcoal and **b** coke

at similar d-spacings, therefore it could be possible that a spinel without chromium is responsible for the measured intensities in the reduced samples. The observed forsterite peaks are weak in the raw ore and in the samples reduced at 1000 °C. In the samples reduced at higher temperatures, they become stronger, this is in line with the thermochemical simulation, that predicts an increasing amount of an olivine phase rich in Mg_2SiO_4. Peaks of the selected FeCr phase are already slightly visible at samples treated at 1000 °C, which was also predicted by the thermochemical simulation. Increasing the temperature leads to a slight increase in the intensity of the FeCr peaks. The majority of new peaks compared to the raw ore in the reduced samples at 1150 and 1300 °C can be explained by a chromium carbide phase, which has a relatively high intensity. Therefore, it can be assumed that the majority of pre-reduction does not result in the formation of a metallic phase, but rather a carbide phase instead.

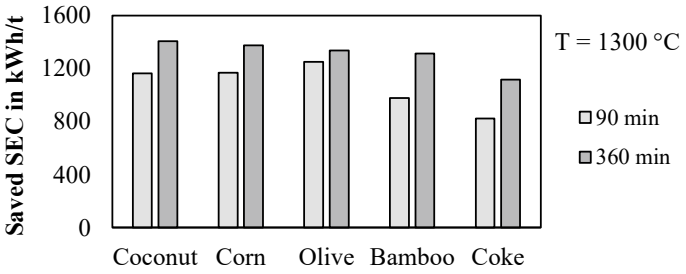

Fig. 7 Saved specific electrical energy consumption due to the pre-reduction at 1300 °C

Influence of the Pre-Reduction on the Specific Electrical Energy Consumption

Assuming, that the degree of reaction as calculated by Eq. 5 can be used to calculate the specific electrical energy consumption (SEC), the saved SEC in the subsequent smelting process can be calculated by Eq. 1. This is shown in Fig. 7 for the five reducing agents used at 1300 °C for the pre-reduction and for reaction times of 90 and 360 min.

It is clearly visible that any pre-reduction process results in a decrease of SEC. The highest decrease in SEC with 1373.8 kWh/t is possible with coconut charcoal at 360 min holding time. The lowest decrease of SEC with 822.0 kWh/t can be reached using coke as a reducing agent at 60 min holding time. The mean SEC savings in percent were 40% for the bio-based reducing agents and 32.8% for coke after 360 min.

Conclusion

The pre-reduction of chromite followed by the smelting in a submerged arc furnace is currently the industrial production route with the lowest specific electrical energy consumption. However, fossil carbon carriers are used as a reducing agent in this process, and this leads to direct CO_2 emissions. To decrease the specific CO_2 emissions for the production of ferrochrome, the suitability of bio-based reducing agents as an alternative to coke was investigated. In this work, the pre-reduction of chromite by several reducing agents was carried out for varying temperatures, reaction times, and carbon additions. While at 1000 and 1150 °C the degree of reaction was rather low, a reaction temperature of 1300 °C yielded a maximum degree of reaction up to 65.4% using coconut shell charcoal as a reducing agent, followed by corn cob charcoal with 63.9%, olive pomace charcoal with 62.1%, bamboo charcoal with 61.0%, and lignite coke with 51.9%. Especially after longer reaction times, the degree of reaction of the bio-based reducing agents was relatively similar, while for shorter

durations significant differences in the degree of reaction were observable. The X-ray diffraction analysis of the pre-reduced samples further revealed, that the reaction occurring during the pre-reduction is mostly attributed to the formation of carbides with the stoichiometric formula Cr_7C_3, while the content of metals produced was significantly smaller.

It is estimated, that the pre-reduction of chromite can decrease the specific electrical energy consumption by 40% compared to the direct smelting of chromite. However, there are some issues to overcome before bio-based carbon can be a substitute in an industrial scale. As some samples of bio-based carbon contained significantly higher chlorine and phosphorus contents compared to coke. In the case of chlorine, this could be a challenge for equipment in contact with off-gas, which will likely contain elevated chlorine contents. In the case of phosphorous, this could be an issue regarding the quality of the produced ferrochrome, since phosphorous is an impurity in ferroalloys. Therefore, potential bio-based charcoals have to be carefully selected, to avoid problems due to the chemical composition. The sample with the lowest phosphorous and chlorine content is coconut shell charcoal, which also yielded the highest degree of reaction. One advantage of all bio-based carbon samples is a significantly lower sulfur content compared to fossil coke, which might yield lower sulfur contents in the final alloy and reduced SO_2-emission to the atmosphere.

References

1. Sommerfeld M, Friedrich B (2021) Replacing fossil carbon in the production of ferroalloys with a focus on bio-based carbon: a review. Minerals 11(11):1286. https://doi.org/10.3390/min11111286
2. Fick G, Mirgaux O, Neau P, Patisson F (2014) Using biomass for pig iron production: a technical, environmental and economical assessment. Waste Biomass Valorization 5(1):43–55. https://doi.org/10.1007/s12649-013-9223-1
3. Suopajärvi H, Umeki K, Mousa E, Hedayati A, Romar H, Kemppainen A, Wang C, Phounglamcheik A, Tuomikoski S, Norberg N, Andefors A, Öhman M, Lassi U, Fabritius T (2018) Use of biomass in integrated steelmaking—status quo, future needs and comparison to other low-CO_2 steel production technologies. Appl Energy 213:384–407. https://doi.org/10.1016/j.apenergy.2018.01.060
4. Mousa E, Wang C, Riesbeck J, Larsson M (2016) Biomass applications in iron and steel industry: an overview of challenges and opportunities. Renew Sustain Energy Rev 65:1247–1266. https://doi.org/10.1016/j.rser.2016.07.061
5. Quader MA, Ahmed S, Ghazilla RAR, Ahmed S, Dahari M (2015) A comprehensive review on energy efficient CO_2 breakthrough technologies for sustainable green iron and steel manufacturing. Renew Sustain Energy Rev 50:594–614. https://doi.org/10.1016/J.RSER.2015.05.026
6. Suopajärvi H, Kemppainen A, Haapakangas J, Fabritius T (2017) Extensive review of the opportunities to use biomass-based fuels in iron and steelmaking processes. J Clean Prod 148:709–734. https://doi.org/10.1016/j.jclepro.2017.02.029
7. Rosenfeld DC, Böhm H, Lindorfer J, Lehner M (2020) Scenario analysis of implementing a power-to-gas and biomass gasification system in an integrated steel plant: a techno-economic and environmental study. Renew Energy 147:1511–1524. https://doi.org/10.1016/J.RENENE.2019.09.053

8. Mandova H, Leduc S, Wang C, Wetterlund E, Patrizio P, Gale W, Kraxner F (2018) Possibilities for CO_2 emission reduction using biomass in European integrated steel plants. Biomass Bioenerg 115:231–243. https://doi.org/10.1016/j.biombioe.2018.04.021
9. Suopajärvi H, Pongráczb E, Fabritiusa T (2013) The potential of using biomass-based reducing agents in the blast furnace: a review of thermochemical conversion technologies and assessments related to sustainability. Renew Sustain Energy Rev 25:511–528. https://doi.org/10.1016/j.rser.2013.05.005
10. Gupta RC (2003) Woodchar as a sustainable reductant for ironmaking in the 21st century. Min Proc Ext Met Rev 24(3–4):203–231. https://doi.org/10.1080/714856822
11. Wei R, Zhang L, Cang D, Li J, Li X, Xu CC (2017) Current status and potential of biomass utilization in ferrous metallurgical industry. Renew Sustain Energy Rev 68:511–524. https://doi.org/10.1016/j.rser.2016.10.013
12. Basson J, Daavittila J (2013) High carbon ferrochrome technology. In: Gasik M (ed) Handbook of ferroalloys. Elsevier/Butterworth-Heinemann. Amsterdam, The Netherlands, pp 317–363
13. Kleynhans ELJ, Beukes JP, van Zyl PG, Fick JIJ (2017) Techno-economic feasibility of a pre-oxidation process to enhance prereduction of chromite. J S Afr Inst Min Metall 117(5):457–468. https://doi.org/10.17159/2411-9717/2017/v117n5a8
14. Kleynhans ELJ, Neizel BW, Beukes JP, van Zyl PG (2016) Utilisation of pre-oxidised ore in the pelletised chromite pre-reduction process. Miner Eng 92:114–124. https://doi.org/10.1016/j.mineng.2016.03.005
15. Kleynhans ELJ, Beukes JP, van Zyl PG, Bunt JR, Nkosi NSB, Venter M (2017) The effect of carbonaceous reductant selection on chromite pre-reduction. Metall Mater Trans B 48(2):827–840. https://doi.org/10.1007/s11663-016-0878-4
16. van Staden Y, Beukes JP, van Zyl PG, Ringdalen E, Tangstad M, Kleynhans ELJ, Bunt JR (2018) Damring formation during rotary kiln chromite pre-reduction: effects of pulverized carbonaceous fuel selection and partial pellet melting. Metall Mater Trans B 49(6):3488–3503. https://doi.org/10.1007/s11663-018-1376-7
17. Mohale GTM, Beukes JP, Kleynhans ELJ, van Zyl PG, Bunt JR, Tiedt LR, Venter AD, Jordaan A (2017) SEM image processing as an alternative method to determine chromite pre-reduction. J S Afr Inst Min Metall 117(11):1045–1052. https://doi.org/10.17159/2411-9717/2017/v117n11a9
18. Neizel BW, Beukes JP, van Zyl PG, Dawson NF (2013) Why is $CaCO_3$ not used as an additive in the pelletised chromite pre-reduction process? Miner Eng 45:115–120. https://doi.org/10.1016/j.mineng.2013.02.015
19. Paktunc D, Thibault Y, Sokhanvaran S, Yu D (2018) Influences of alkali fluxes on direct reduction of chromite for ferrochrome production. J S Afr Inst Min Metall 118(12). https://doi.org/10.17159/2411-9717/2018/v118n12a9
20. Sokhanvaran S, Paktunc D, Barnes A (2018) NaOH-assisted direct reduction of Ring of Fire chromite ores, and the associated implications for processing. J S Afr Inst Min Metall 118(6). https://doi.org/10.17159/2411-9717/2018/v118n6a4
21. Yu D, Paktunc D (2018) Kinetics and mechanisms of the carbothermic reduction of chromite in the presence of nickel. J Therm Anal Calorim 132(1):143–154. https://doi.org/10.1007/s10973-017-6936-6
22. Sommerfeld M, Friedrich B (2021) Proposition of a thermogravimetric method to measure the ferrous iron content in metallurgical-grade chromite. Minerals 12(2):109. https://doi.org/10.3390/min12020109
23. Bale CW, Bélisle E, Chartrand P, Decterov SA, Eriksson G, Gheribi AE, Hack K, Jung I-H, Kang Y-B, Melançon J, Pelton AD, Petersen S, Robelin C, Sangster J, Spencer P, van Ende M-A (2016) FactSage thermochemical software and databases, 2010–2016. Calphad 54:35–53. https://doi.org/10.1016/j.calphad.2016.05.002